

Influence of Heterogeneity of Binding Sites of Humic Acid on its Complexation with Actinyl Ions

Shinya NAGASAKI^{1*}, Takumi SAITO², and Satoru TANAKA²

¹Institute of Environmental Studies, The University of Tokyo, Tokyo 113-0033, Japan

²Department of Quantum Engineering and Systems Science, The University of Tokyo, Tokyo 113-8656, Japan

The influence of heterogeneity of binding sites of humic acid was investigated using three different experimental approaches. 1) Complexation with UO_2^{2+} was studied by fluorescence spectroscopy. Considering the quenching phenomena, the apparent stability constants of complexation of humic acid with UO_2^{2+} were evaluated and compared with the values reported in the literature. 2) Complexation kinetics of NpO_2^+ with humic acid and fulvic acid was investigated by kinetic spectra. The complexation kinetics was found to be controlled by the heterogeneity of binding sites. 3) The migration of humic acid- NpO_2^+ complexes was discussed experimentally by column experiments and analytically by a migration model. The concentration profile of NpO_2^+ in the column was qualitatively simulated.

KEYWORDS: humic acid, UO_2^{2+} , NpO_2^+ , heterogeneity, binding site

I. Introduction

Humic substances (HS), which result from the decomposition of plant and animal tissues, are ubiquitous in the environment, occurring in soils, waters, and sediments of the ecosphere. They are polyelectrolytes, and their functional groups, their size, structure, and composition are heterogeneously distributed, depending on their origins and environmental conditions¹⁾. HS are also recognized to play important roles in the environmental behavior of inorganic or organic materials. In case of inorganics, such as heavy metals and radionuclides, HS form stable complexes with them that change their geochemical properties, including mobility, solubility and oxidation states^{2,3)}. Many researchers have investigated such complexation behavior using ultrafiltration⁴⁾, ion exchange^{4,5)}, ion selective electrode potentiometry⁶⁾, all of which are the methods accompanying the separation between the complexed and the free metal ions. In contrast, several spectroscopic techniques, such as fluorescence spectroscopy, are recognized to be useful for the evaluation of the complexation between HS and metal ions, because they can directly probe the states of the functional groups in HS. In our previous paper⁷⁾, we indicated the presence of two complexing components in Aldrich humic acid (HA) by quenching of the fluorescence of HA with UO_2^{2+} , followed by spectral deconvolution using SIMPLISMA. This means that the chemical and geochemical behavior of metal ions is influenced by the heterogeneity of binding sites of HA. Recently, there has been a consensus of the wide heterogeneity of binding energetics in the HA, and the importance of heterogeneity for sorption of metal ions has been pointed out. This heterogeneity is due to the change of conformation of the binding sites, due to the different chemical nature and steric environment of the binding sites and due to the variation of the electrostatic potential by the complexation in the neighborhood of the binding sites.

HA are the important components of groundwater colloids.

As mentioned above, the binding properties of HA are not uniform. Their affinity and accessibility for metal ions may vary depending on (i) the different charge density, (ii) the location of binding sites, and (iii) the shape of HA. These properties give rise to a heterogeneity of binding sites of HA, influencing their binding properties with respect to metal ions.

In the present paper, the influence of heterogeneity of binding sites of HA was investigated using three different experimental approaches.

Firstly, we clarified the relationship between the complexing components obtained by SIMPLISMA and the structure of HA, and identify the major fractions contributing to the quenching of the fluorescence of HA with UO_2^{2+} . For this purpose, HA was fractionated by means of GPC (gel permeation chromatography), and the complexation behavior of each fraction with UO_2^{2+} was examined by fluorescence spectroscopy and SIMPLISMA analysis.

Secondly, the complexation kinetics of NpO_2^+ with HA was investigated by the kinetic spectra method, and the influence of heterogeneity of HA on the complexation with NpO_2^+ is discussed.

Thirdly, the migration of NpO_2^+ associated with HA was studied by column experiments packed with quartz powder and the concentration profile of NpO_2^+ in the column was simulated analytically.

II. Experimental

1. Complexation of HA with UO_2^{2+}

HA was purchased from Aldrich Co. (Germany), purified according to the literature, and then stored in a desiccator under vacuum. This purified HA was fractionated using GPC in the similar way as described in the literature⁸⁾. HA was dissolved in 5×10^{-2} M Na_2HPO_4 , and injected into the Sephadex G-50 column (26mm i.d. and 700mm height), and then eluted with phosphate buffer (1×10^{-3} M, pH = 8.00)

*Corresponding Author: Phone: +81-3-5841-6995,

Fax: +81-3-5841-8622, e-mail: nagasaki@k.u-tokyo.ac.jp

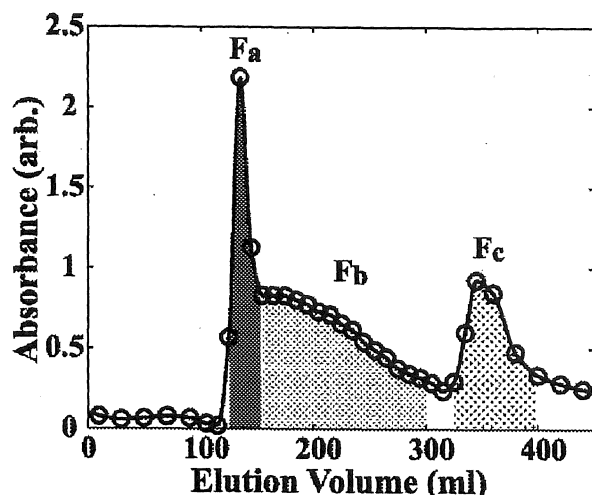


Fig. 1 Gel permeation chromatogram of humic acid. Column size: 26 mm i.d. \times 700 mm height; 10 ml aliquot of 1g/l HA; eluent: 1×10^{-3} M phosphate buffer (pH = 8); flow rate: 1 ml/min; UV detection wavelength: 254nm.

at a flow rate of 1ml/min using a cassette tube pump (Iuchi, Japan). The fractionated samples were detected at 254nm using UV-3100 (Shimadzu, Japan), and finally collected by an Advantec SF-2120 fraction collector. A chromatogram of HA is shown in Fig. 1, and the three fractions were obtained according to the peaks in Fig. 1, F_a , F_b and F_c . In GPC, the faster a fraction is eluted, the larger the molecular weight, and the molecular weight of the obtained fractions were: $F_a > F_b > F_c$. The solutions containing the fractionated HA were evaporated under reduced pressure, and precipitated with HCl (pH = 1). After removing salts by dialysis, the fractionated HA powders were obtained by drying under vacuum.

A series of HA stock solutions (20ml), unfractionated HA (UHA) and its three fractions with a concentration of 10mg/l, was collected in the glass vials and the uranyl solution was added with a set of final concentrations ranging from 0 to 1.0×10^{-4} M. The pH and ionic strength of all samples were adjusted to 4.00 ± 0.02 with HClO_4 and NaOH, and 0.1M with NaClO_4 , respectively. Fluorescence spectroscopy was performed using a F-4500 fluorescence spectrometer (HITACHI Co., Japan).

The synchronous fluorescence spectra, which were successively quenched according to the addition of UO_2^{2+} , were resolved by their fluorescence intensity profiles of the extracted complexing components, and the corresponding spectra by SIMPLISMA developed by Windig and Guilment⁹. At the same time, the complexation parameters of the components, the apparent stability constants ($\log K_{app}$) and the concentration of sites (C_L), were evaluated based on these intensity profiles, using nonlinear least-squares techniques of the Multisite Ryan-Weber Model (MSRW)¹⁰.

2. Complexation kinetics of NpO_2^+ with HA

All chemicals except the ^{237}Np solution were reagent grade and used without further purification (Wako Pure Chemical Industries Co. Ltd., Japan). Water was prepared from doubly distilled water by further purification with a Milli-Q system (Millipore); it was ultrafiltered through a 2 nm pore size ultrafilter (UFP1, Millipore) immediately before use. Neptunium-237 in 1M HNO_3 was purchased from LMRI, France. By repeatedly extracting the Np solution with CMPO (*n*-octyl(phenyl)-*N,N*-diisobutylcarbamoylmethylphosphine oxide), a Np(V) stock solution was prepared. The pH of Np stock solution was adjusted with NaOH to pH 6. The pH was measured with a combination glass electrode (type ROSS, Orion Co. Ltd.) calibrated against pH buffer solutions. 1×10^{-2} M NaNO_3 was added to the Np(V) stock solution as the background electrolyte. The concentration of Np(V) stock solutions was 1×10^{-3} M. The oxidation state of Np was spectroscopically confirmed to be pentavalent.

We used Aldrich HA and HA and fulvic acid (FA) purchased from International Humic Substances Society (IHSS), after purification and protonation. 10mg/L of Aldrich HA, IHSS HA or IHSS FA and 1×10^{-5} M NpO_2^+ aqueous solution were mixed by stopped flow method. We investigated the dependence of the sorption kinetics as a function of pH (pH = 4, 5 and 6) at 25 °C. Ionic strength of the solutions was adjusted to $I = 0.1$ M by NaClO_4 . When Np is complexed with HA and FA, the absorbance at 981 nm of NpO_2^+ decreases. After the mixing of the Np(V) solution with HA or FA solutions, the variation of absorbance at 981 nm with time was measured spectrophotometrically.

3. Migration of HA complexes with NpO_2^+

A column used had an inner diameter of 5 mm and was filled with the quartz powder (diameter = 8 μm) up to a height of 300 mm. The porosity of the column was found to be 40 % from the breakthrough phenomenon of non-sorbing tracer, HTO (tritiated water; $T \equiv {}^3\text{H}$). Temperature of the column was controlled at 25 ± 1 °C by a water jacket. The quartz powder used was supplied from APPIE (Association of Powder Process Industry and Engineering, Japan) and immersed in 0.1 M NaClO_4 solution (pH = 6) for more than one year. The detailed characterization of the quartz powder is described elsewhere¹¹.

A feed solution of Np-bearing Aldrich HA was prepared by adding Np solution (1×10^{-5} M) into the HA solution (10 mg/dm³). At C_L is about 10^{-6} M, there are Np-HA and NpO_2^+ present. The pH and I of the feed solution were adjusted to pH = 6 (NaOH) and $I = 0.1$ M (NaClO_4). The salt solution (pH = 6, $I = 0.1$ M) was continuously pumped through the column at the flow velocity of 3×10^{-2} ml/h (i.e. 1.1×10^{-6} m/s), before the feed solution was injected. After pre-equilibrium in the column is achieved by this procedure, the feed solution of Np-HA complexes (two ml) was

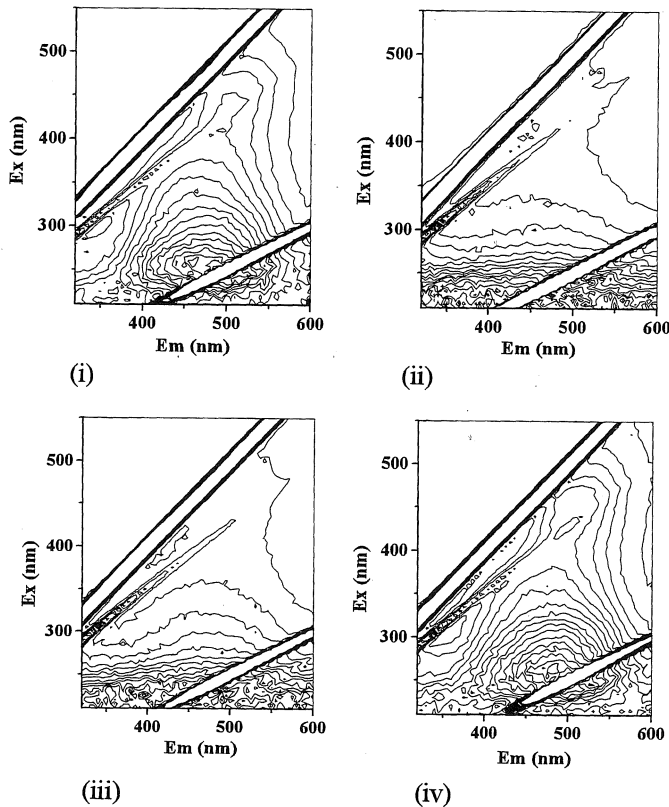


Fig. 2 3D fluorescence spectroscopy of humic acid and its fractions: (i) unfractionated humic acid, (ii) F_a , (iii) F_b and (iv) F_c .

introduced into the column. The concentration of Np in eluate fractions and the concentration profile of Np in the column were determined by γ counting. We also measured the NpO_2^+ migration in the column in the absence of HA and the latex particles (diameter = 50 nm, 100 nm, 450 nm and 1 μm). The concentration of latex particles was determined spectroscopically¹².

III. Results and discussions

1. Complexation of HA with UO_2^{2+}

1.1 3D fluorescence spectroscopy

The 3D fluorescence spectra of UHA and the three fractions are shown in Fig. 2. Two peaks in the spectrum of UHA (Fig. 2(i)), 450/520nm (excitation/emission wavelength) and 250/475nm, were recognized in that of F_c (Fig. 2(iv)). On the other hand, the spectra of F_a and F_b (Figs. 2(ii) and (iii)) had no distinct peaks. Therefore, most of the fluorescence of UHA is considered to result from that of F_c , which has the lowest molecular weight. Aoyama et al.¹³ investigated the spectroscopic properties of fractionated HA and concluded that 'fluorescent substances' were rich in lower molecular weight compounds. Fukushima et al.¹⁴ also concluded that the largest amounts of acidic groups were found in the lowest molecular fraction. Hence, the fluorescence of Aldrich HA is considered to relate to the structure, which has low molecular weight and a lot of

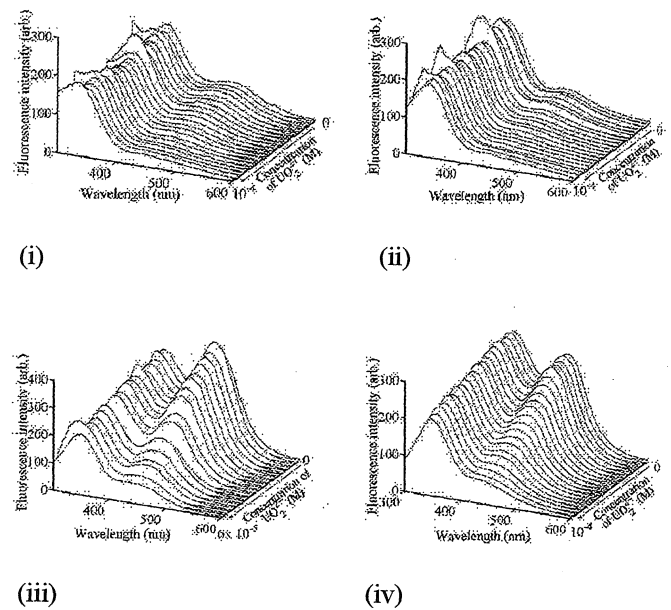


Fig. 3 Quenching profile of (i) unfractionated humic acid, (ii) F_a , (iii) F_b and (iv) F_c . pH = 4.00 and ionic strength 0.1M.

functional groups, mostly carboxylic and phenolic groups.

1.2 Quenching analysis

The quenching profiles of UHA and the three fractions, as a function of the concentration of UO_2^{2+} , are shown in Fig. 3. The fluorescence of F_a and F_b was slightly quenched in the region of wavelength from 400nm to 600nm. However, it was difficult to apply SIMPLISMA for deconvoluting the quenching profiles. On the other hand, the quenching tendency of F_c was similar to that of UHA, which agreed with the results of 3D fluorescence spectroscopy. These two quenching profiles were deconvoluted into the fluorescence intensity profiles and the spectra of components using SIMPLISMA, as shown Figs. 4 (i)-(iv). It is clear that the first component (solid line), which has a peak around 450nm, was more strongly quenched with UO_2^{2+} than the second component (dashed line), which has one around 350nm. From the fluorescence intensity profiles, the complexation parameters, the apparent stability constant ($\log K_{app}$) and the concentration of site (C_L), were evaluated by fitting to MSR model. The obtained parameters are listed in Table 1. The apparent stability constants of F_c were 5.05 for the first component and 4.58 for the second one. These values were similar to those evaluated for UHA, but the site concentrations obtained for the two components were different between UHA and F_c . F_c contained more sites for the second component than that for the first component. On the other hand, UHA contained more sites for the first component. This may result from the contribution of F_a and F_b , which have the fluorescent components quenched around 450nm. However, the detail of their contribution has been unknown, since the mixture of the fractions could affect the total fluorescence properties,

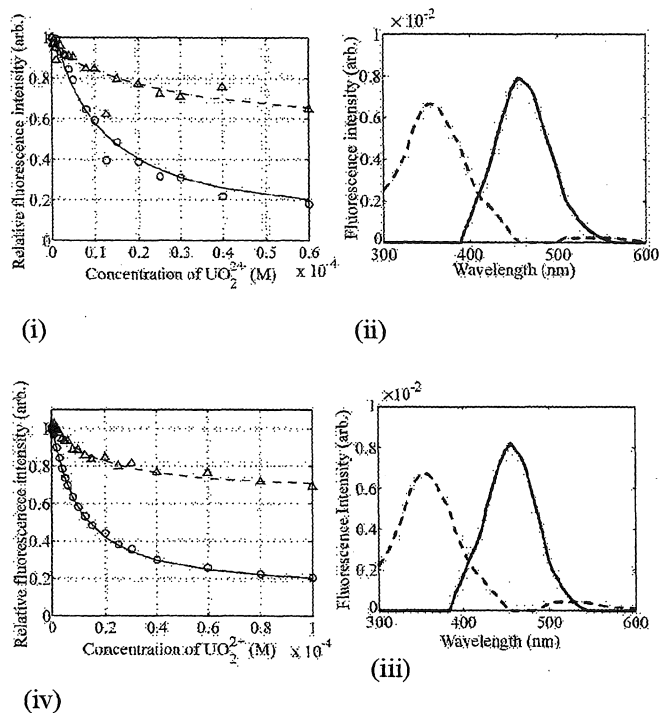


Fig. 4 Result of the curve resolution of quenching profile of unfractionated humic acid (i, ii) and F_c (iii, iv) with SIMPLISMA

Table 1 Apparent stability constants and site concentration of the first and second components of UHA and F_c

	$\log K_{app1}$	$\log K_{app2}$	C_{L1} (M)	C_{L2} (M)
UHA	5.07	4.70	2.24×10^{-6}	1.28×10^{-6}
F_c	5.05	4.58	1.27×10^{-6}	2.74×10^{-6}

that is, the fluorescence of UHA is not always the arithmetic mean of that of the fractions, as pointed out by Fukushima et al.¹⁵⁾ At the same time, the presence of the complexing sites, which do not contribute to fluorescence of HA, is not taken into account in the quenching analysis. Especially, the apparent stability constants evaluated here are smaller than the literature values⁴⁾. Therefore, the contribution of the high molecular weight fractions to the complexation with UO_2^{2+} has to be further investigated.

2. Complexation kinetics of NpO_2^+ with HA

Assuming that the complexation of NpO_2^+ with HA and FA is a pseudo-first-order reaction, the kinetics at each binding site Z_i of HA and FA is described as

$$n_i(t) = n_i^0 [1 - \exp(-k_i t)] \quad (1)$$

where $n_i(t)$ is the concentration of binding site Z_i complexed with NpO_2^+ at time t , n_i^0 the total concentration of binding site Z_i complexed with NpO_2^+ at equilibrium, and k_i the apparent complexation rate constant at Z_i . Eq.(1) is

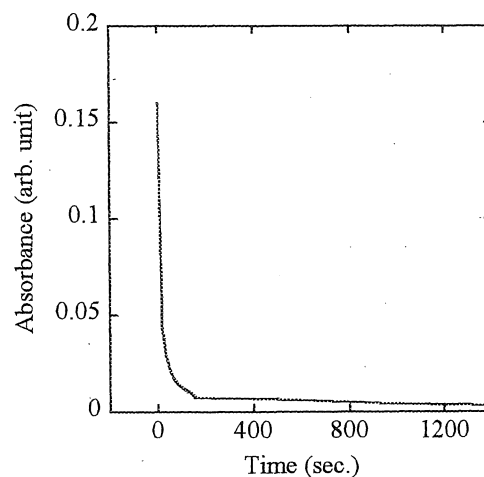


Fig. 5 Decrease in absorbance of NpO_2^+ at pH = 7

rearranged to Eq.(2) with $\Delta n_i(t) = n_i^0 - n_i(t)$

$$\Delta n_i(t) = n_i^0 \exp(-k_i t) \quad (2)$$

We can not experimentally observe the complexation reaction at each site Z_i , but can observe the time dependence of change in total NpO_2^+ concentration $\Delta n(t)$. If the number n is large enough, the sum may be replaced by an integral as follows

$$\Delta n(t) = \sum_i^n \Delta n_i(t) = \sum_i^n n_i^0 \exp(-k_i t)$$

$$\Delta n(t) = F \int_0^\infty A(k) \exp(-k_i t) dk$$

where F is the proportionality factor and $A(k)$ represents the distribution of sites, complexed with Np , as a function of rate constant k , specific for each site. The $A(k)$ plotted vs. $\log k$ gives the kinetic spectrum¹⁶⁾. The $A(k)$ is obtained by an inverse Laplace transform on $n(t)$ which can be experimentally obtained from the change in the absorbances at 981 nm with time. In the present work, the inverse Laplace transform was numerically carried out, according to the Talbot method.

Figure 5 shows the decrease of absorbance at pH = 7 for Aldrich HA. We can see the first decay and consequent slow decay. If we try to fit the discrete model to the decay curve, 5 components should be considered at least. By fitting the above spectrum method, the heterogeneity of binding sites of HA and FA were studied. The complexation kinetic spectrum at pH = 7 calculated from the decay curve of Fig. 5 is shown in Fig. 6. It was found that the heterogeneity of binding sites is widely distributed, meaning that a continuous distribution of rate constants may be needed to adequately model the complexation of HA with

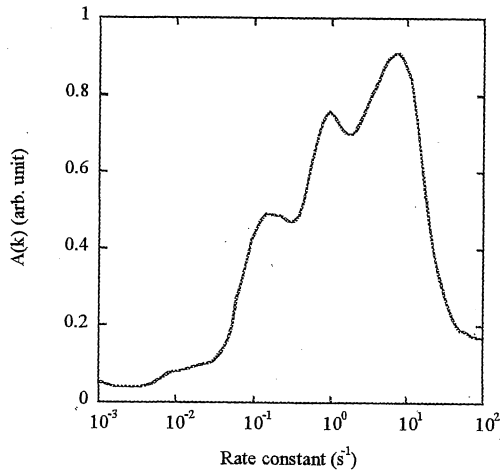


Fig. 6 Kinetic spectrum of complexation of Aldrich HA with NpO_2^+ at pH = 7

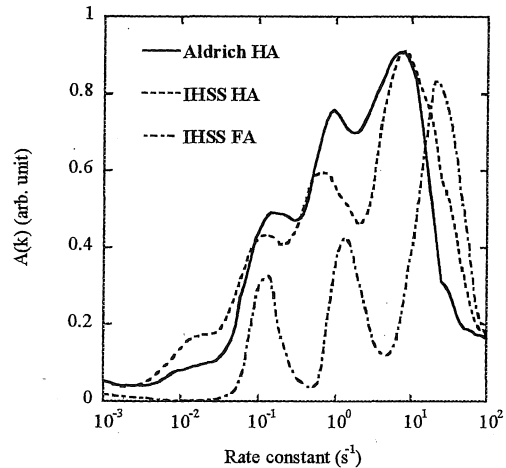


Fig. 8 Complexation kinetic spectra of Aldrich HA, IHSS HA and IHSS FA

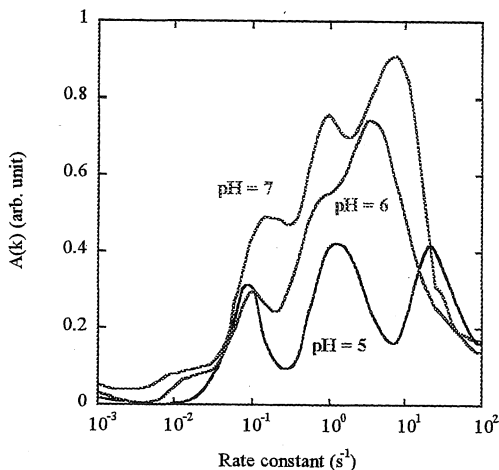


Fig. 7 pH dependence of kinetic spectra of Aldrich HA

NpO_2^+ . Dependence of spectrum on pH is illustrated in Fig. 7. At low pH, heterogeneity of binding sites was relatively small, but as pH increases, it became remarkable. As pH decreases, agglutination of HA takes place and contact with interior binding sites is blocked. On the other hand, as pH increases, humic molecular mass opens to facilitate more contact with NpO_2^+ . Hence, NpO_2^+ can be associated with binding sites located in interior. Figure 8 shows the kinetic spectra of Aldrich HA, IHSS HA and IHSS FA. Compared with the spectra of HA, FA showed the three resolved regions. This may be due to the lower molecular mass of FA. It was also found that the region of slow rate constant reduced for FA. This is because the number of interior binding sites is small.

3. Migration of HA complexes with NpO_2^+

3.1 Breakthrough of latex particles

Breakthrough behavior of latex particles was dependent

on their size, but generally speaking, we found that more than 50 % of latex particles were eluted as fast as HTO and that some fraction of latex particles were trapped in the column by the filtration effect because the latex particles are not retained by sorption on the quartz powder.

In our previous work¹⁷⁾, we developed the colloid migration model considering the filtration effect and also simulated the Np-colloid migration observed in column experiments by using this model. In the present work, by fitting the colloid migration model to the breakthrough curves of latex particles, the filtration coefficient of each latex particle was evaluated. Filtration coefficients evaluated are summarized in Fig. 9. It was found that the filtration coefficient decreased with increasing the particle size, had a minimum value and then increased. The reason for this tendency is not clear, but we considered that the smaller particles had more chances to collide with the quartz surface and intrude into the narrow flow paths and then trapped by filtration, and that the larger particles were filtered out due to their own size.

3.2 Concentration profile of Np

The concentration profiles of NpO_2^+ in the column at $V(i)/V_{eff} = 3$ and 8 were plotted in Fig. 10. $V(i)$ is the volume of effluent solution passing through the column and V_{eff} is the effective pore volume in the column. In this figure, the concentration of Np means the sum of Np in the liquid phase and Np sorbed/trapped on the quartz powder. It was found that the concentration of Np monotonously decreased with the migration distance. Taking into account the advection-diffusion theory, the concentration profiles were successfully fitted as shown by solid lines in Fig. 10.

The concentration profiles of Np-HA complexes in the column at $V(i)/V_{eff} = 0.5$ and 1.5 were plotted in Fig. 11. It was found that the concentration of Np monotonously decreased in the column inlet, then showed the plateau region and again decreased.

By using the colloid migration model, we tried to simulate the Np concentration profiles. As a preliminary

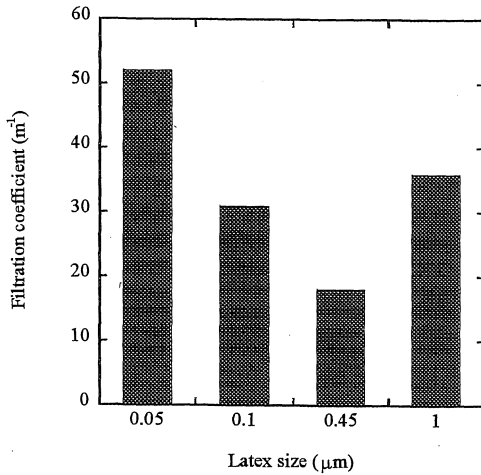
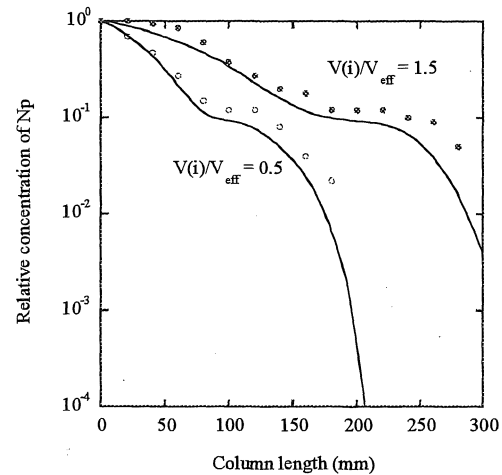


Fig. 9 Dependence of filtration coefficient on latex size



column

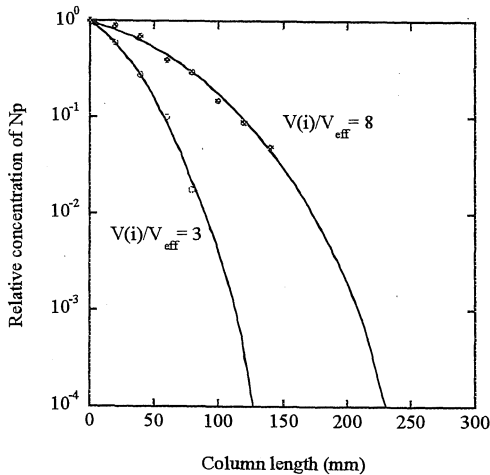


Fig. 10 Concentration profiles of NpO_2^+ in the column

consideration in the present work, we made some assumption as follows:

- (1) Np-HA complexes were not sorbed on the quartz powder,
- (2) Np-HA migrated by advection together with the effluent solution,
- (3) the initial size distribution of Np-HA complexes was stable and did not change during the migration, and
- (4) the filtration coefficients of latex particles could be used to those of Np-HA, as the size and structure and the interaction of complexes are quite different those of latex particles as mentioned below.

The size fractionation of Np-HA complexes measured by filtration is shown in Table 2. Size range divisions measured for the latex particles were not identical to those of complexes, due to the lack of commercially available filter pore sizes. In the present work, as the 0th approximation, the filtration coefficient values of 0.05 μm, 0.1 μm, 0.45 μm and 1 μm latex particles were used as those of Np-HA

Table 2 Size fractionation and filtration coefficient of Np-HA

Size (μm)	Fractionation (%)	Filtration coefficient (m ⁻¹)
< 0.1	10	52
0.1 ~ 0.2	56	31
0.2 ~ 0.8	22	18
> 0.8	12	36

complexes of smaller than 0.1 μm, 0.1 ~ 0.2 μm, 0.2 ~ 0.8 μm and larger than 0.8 μm as shown in Table 2. Calculation results are illustrated as solid lines in Fig. 11. It was found that the Np concentration profiles qualitatively agreed with the experimental results, but did not quantitatively agree. Especially, the calculation predicted smaller Np concentrations in the all column regions, compared with the experimental results.

As mentioned above, we had some assumptions in the calculation. However, Np-HA complexes can be sorbed on the quartz powder and the affinity depends on the size of complexes, the dispersion of complexes may be important, the size distribution of complexes may change during the migration, and the filtration coefficient values of complexes are not identical to those of latex particle. Therefore, we have to make much effort to understand the migration of Np-HA complexes and to develop a quantitative migration model which is based on the laws of physics and chemistry.

IV. Conclusions

We studied the influence of heterogeneity of binding sites of HA on complexation with UO_2^{2+} and complexation kinetics with NpO_2^+ and the migration of Np-HA complexes in column experiments. The following conclusions have been drawn.

- (1) Combination of Synchronous fluorescence spectroscopy with SIMPLISMA method shows the heterogeneity of carboxylic functional groups in humic acids.
- (2) Kinetic spectrum gives the information on heterogeneity of binding sites of humic acids.
- (3) Colloid size influences the filtration behavior. The dependence of filtration coefficient on colloid size should be evaluated, together with consideration of heterogeneity of interaction sites of humic acids with solid phases and the heterogeneity of sorption kinetics.

References

- 1) W. Ziechmann, W., Evolution of Structural Models from Consideration of Physical and Chemical Properties. In: *Humic Substances and their Role in the Environment* (F. H. Frimmel, R. F. Christian, eds.). John Wiley & Sons, New York, 1988.
- 2) P.R. Wittbrodt and C.D. Palmer, *Environ. Sci. Technol.* **29**(1995)255-263.
- 3) A. Lui and R.D. Gonzales, *J. Colloid Interface Sci.* **218**(1999)225-232.
- 4) K.R. Czerwinski, G. Buckau, F. Scherbaum and J.I. Kim, *Radiochim. Acta* **65**(1994)111-119.
- 5) H. Geckeis, T. Rabung and J.I. Kim, J. I.: Effect of Humic Substances on the Migration of Radionuclides: Complexation and Transport of Actinides. In: *2nd Technical Progress, EC Project* (G. Buckau, eds.), Forschungszentrum Karlsruhe, 1999.
- 6) P. Lubal, D. Fetsch, D. Siroky, M. Lubalova, J. Senkyr and J. Havel, *Talanta* **51**(2000)977-991.
- 7) T. Saito, S. Nagasaki and S. Tanaka, *Radiochim. Acta* (in press).
- 8) M. Fukushima, S. Tanaka, H. Nakamura and S. Ito, *Talanta* **43**(1996)383-390.
- 9) W. Windig and J. Guilment, *Anal. Chem.* **63**(1991)1425-1432.
- 10) D.S. Smith and J.R. Kramer, *Anal. Chim. Acta.* **416**(2000)211-220.
- 11) S. Nagasaki, S. Tanaka and A. Suzuki, *J. Nucl. Sci. Technol.*, **31**(1994)143-150.
- 12) S. Nagasaki, S. Tanaka and A. Suzuki, *J. Nucl. Sci. Technol.*, **30**(1993)1136-1144.
- 13) M. Aoyama, A. Watanabe and S. Nagao, S.: Characterization of the "Fluorescence Fraction" of Soil Humic Acids. In: *Humic substances: Versatile Components of Plants, Soil and Water* (Ghabbour, E. A. and Davis, G. eds.). The Royal Society of Chemistry, Cambridge, 125 (2000).
- 14) S. D. Killops and V. J. Killops, *Organic Geochemistry*, John Willey, New York (1993) 95-106.
- 15) M. Fukushima, S. Tanaka, H. Nakamura and S. Ito, *Anal. Chim. Acta.* **322**, (1996)173-185.
- 16) A. Pohlmeier, *Progr. Colloid and Polym. Sci.*, **95**(1994)113-118.
- 17) S. Nagasaki, T. Nakatsuka, S. Tanaka and A. Suzuki, *J. Nucl. Sci. Technol.*, **31**(1994)623-625.